NASA/TM–2005–212794

Laser Frequency Stabilization for LISA

Guido Mueller, Paul McNamara, Ira Thorpe, and Jordan Camp

December 2005

The NASA STI Program Office … in Profile

Since its founding, NASA has been dedicated to the advancement of aeronautics and space science. The NASA Scientific and Technical Information (STI) Program Office plays a key part in helping NASA maintain this important role.

The NASA STI Program Office is operated by Langley Research Center, the lead center for NASA's scientific and technical information. The NASA STI Program Office provides access to the NASA STI Database, the largest collection of aeronautical and space science STI in the world. The Program Office is also NASA's institutional mechanism for disseminating the results of its research and development activities. These results are published by NASA in the NASA STI Report Series, which includes the following report types:

- TECHNICAL PUBLICATION. Reports of completed research or a major significant phase of research that present the results of NASA programs and include extensive data or theoretical analysis. Includes compilations of significant scientific and technical data and information deemed to be of continuing reference value. NASA's counterpart of peer-reviewed formal professional papers but has less stringent limitations on manuscript length and extent of graphic presentations.
- TECHNICAL MEMORANDUM. Scientific and technical findings that are preliminary or of specialized interest, e.g., quick release reports, working papers, and bibliographies that contain minimal annotation. Does not contain extensive analysis.
- CONTRACTOR REPORT. Scientific and technical findings by NASA-sponsored contractors and grantees.
- CONFERENCE PUBLICATION. Collected papers from scientific and technical conferences, symposia, seminars, or other meetings sponsored or cosponsored by NASA.
- SPECIAL PUBLICATION. Scientific, technical, or historical information from NASA programs, projects, and mission, often concerned with subjects having substantial public interest.
- TECHNICAL TRANSLATION. English-language translations of foreign scientific and technical material pertinent to NASA's mission.

Specialized services that complement the STI Program Office's diverse offerings include creating custom thesauri, building customized databases, organizing and publishing research results . . . even providing videos.

For more information about the NASA STI Program Office, see the following:

- Access the NASA STI Program Home Page at http://www.sti.nasa.gov/STI-homepage.html
- E-mail your question via the Internet to help@sti.nasa.gov
- Fax your question to the NASA Access Help Desk at (301) 621-0134
- Telephone the NASA Access Help Desk at (301) 621-0390
- Write to:
  NASA Access Help Desk
  NASA Center for AeroSpace Information
  7121 Standard Drive
  Hanover, MD 21076–1320

NASA/TM–2005–212794

Laser Frequency Stabilization for LISA

Guido Mueller and Ira Thorpe
Department of Physics, University of Florida, Gainesville, Florida

Paul McNamara and Jordan Camp
NASA/Goddard Space Flight Center, Greenbelt, Maryland

National Aeronautics and
Space Administration

Goddard Space Flight Center
Greenbelt, Maryland 20771

December 2005

Available from:

NASA Center for AeroSpace Information
7121 Standard Drive
Hanover, MD 21076-1320
Price Code: A17

National Technical Information Service
5285 Port Royal Road
Springfield, VA 22161
Price Code: A10

Laser frequency stabilization for LISA

Guido Mueller[1], Paul McNamara[2], Ira Thorpe[1], Jordan Camp[2]

[1]Department of Physics, University of Florida, Gainesville, FL 32611

[2]Goddard Space Flight Center, Greenbelt, Md, 20771

Abstract

The requirement on laser frequency noise in the Laser Interferometer Space Antenna (LISA) depends on the velocity and our knowledge of the position of each spacecraft of the interferometer. Currently, it is assumed that the lasers must have a prestabilized frequency stability of $30\,\mathrm{Hz}/\sqrt{\mathrm{Hz}}$ over LISA's most sensitive frequency-band (3 mHz to 30 mHz). The intrinsic frequency stability of even the most stable commercial lasers is several orders of magnitude above this level. Therefore, it is necessary to stabilize the laser frequency to an ultrastable frequency reference which meets the LISA requirements. The baseline frequency reference for the LISA lasers are high finesse optical cavities based on ultralow expansion glass (ULE) spacers. We measured the stability of two ULE spacer cavities with respect to each other. Our current best results show a noise floor at, or below, $30\,\mathrm{Hz}/\sqrt{\mathrm{Hz}}$ above 3 mHz. In this report, we describe the experimental layout of the entire experiment and discuss the limiting noise sources.

1 Introduction

The Laser Interferometer Space Antenna (LISA) [1], is a joint ESA/NASA mission designed to measure low-frequency gravitational radiation emitted from distant super massive black hole binaries and mergers, from galactic neutron star and white dwarf binaries, and from super massive black holes capturing neutron stars or smaller black holes. Gravitational waves, first predicted by Einstein, are a direct consequence of the theory of general relativity. Large accelerated masses emit gravitational waves and studying these waves is equivalent to studying the acceleration of these masses.

LISA consists of three spacecraft (s/c) in a heliocentric orbit. The s/c are in a triangular constellation with an armlength of $5 \cdot 10^9$ m. Two inertial proof masses within each spacecraft form the ends of the interferometer arms. The simplest picture is to imagine that one spacecraft acts like a beam splitter in a conventional Michelson interferometer, while the two other spacecraft are the end mirrors. The interferometer measures relative changes in the distances between the beam splitter and the end mirrors. If the lengths of the interferometer arms are not equal, the accuracy of a direct interferometric measurement of the phase difference between the two return beams is limited by laser frequency noise. A technique called "time delay interferometry" is proposed to cancel up to seven orders of magnitude of laser frequency noise by post-processing the data streams to artificially equalize the armlengths. This technique relaxes the requirements on laser frequency noise to [2]

$$\delta\nu < \frac{30\,\mathrm{Hz}}{\sqrt{\mathrm{Hz}}} \qquad \text{at } 3 \text{ mHz}. \tag{1}$$

The frequency reference for the LISA lasers will be a monolithic optical cavity made from three mirrors bonded to a piece of Ultra Low Expansion Glass (ULE) [3]. ULE has a thermal expansion coefficient of less than $2 \cdot 10^{-8} \mathrm{K}^{-1}$ at temperatures between 5 to 35° C. Alternatives to ULE are Zerodur from Schott [4] and Clearceram-Z from Ohara [5] which have similar expansion coefficients. The optical path length (OPL) inside the cavity, and therefore the resonant frequency, depends only on the geometrical stability of the ULE spacer and the bonds between the mirrors and the spacer. The temperature stability of the optical bench inside the spacecraft is expected to be better than $\mu\mathrm{K}/\sqrt{\mathrm{Hz}}$ at frequencies above 1 mHz. If the OPL is limited by the thermal stability of the spacer, the relative length stability $\delta L/L$ of a cavity of length L in such an environment is:

$$\frac{\delta L}{L} < \frac{2 \cdot 10^{-8}}{\mathrm{K}} \cdot \frac{\mu\mathrm{K}}{\sqrt{\mathrm{Hz}}} = \frac{2 \cdot 10^{-14}}{\sqrt{\mathrm{Hz}}} \,. \tag{2}$$

The absolute frequency change $\delta\nu$ of the resonance frequency ν is then:

$$\delta\nu = \frac{\delta L}{L}\nu < \frac{2 \cdot 10^{-14}}{\sqrt{\mathrm{Hz}}} 3 \cdot 10^{14}\,\mathrm{Hz} = \frac{6\,\mathrm{Hz}}{\sqrt{\mathrm{Hz}}} \,. \tag{3}$$

Obviously, every additional factor in frequency noise reduction will either increase the margin or can help to relax other requirements like timing and arm length knowledge (ranging) requirements. In this paper, we will present results that meet LISA's frequency noise requirements of $30\,\mathrm{Hz}/\sqrt{\mathrm{Hz}}$ above 3 mHz. In the following section, we describe the principles of the Pound-Drever-Hall (PDH) [6] technique, which we use to stabilize the laser frequency to the resonant frequency of an optical cavity. The third section gives important details about the experimental setup. In the fourth section, we will discuss potential noise sources. The final section describes the measured frequency noise and puts them in context with the measured noise sources and LISA requirements.

2 Frequency Stabilization with a Reference Cavity

Frequency stabilization systems require a reference frequency and a readout system that utilizes the full stability of the reference frequency. The two most common types of reference frequencies that are used in the optical frequency domain are molecular or atomic transitions and optical cavities. Molecular or atomic transitions like transitions between rotational and vibrational eigenstates of the iodine molecule are especially advantageous if the absolute frequency and the long term frequency stability are of particular interest. Optical cavities based on ultralow expansion materials in temperature stable environments are especially useful in experiments where the short term frequency stability is important. The cross over between these systems is around measurement times of a few seconds to minutes corresponding to signal frequencies between 10 mHz and 1 Hz [7]. The baseline design of the LISA mission uses optical cavities as frequency references for their lasers because of their simplicity and simple readout systems.

Optical cavities for laser frequency stabilization are usually either two-mirror linear cavities or three-mirror triangular cavities. One advantage of linear cavities is the reduced

number of mirrors and subsequently, a reduced number of lossy reflections per roundtrip. The much simpler support structure - a rod with one drilled bore compared to a triangular structure with three bore holes - also reduces the cost of linear cavities. One advantage of triangular cavities is that the reflected beam is automatically separated from the incoming beam and can be directly detected without any additional optical components. Unfortunately, this advantage also makes it more difficult to align triangular cavities compared to linear cavities where the orientation of the reflected beam with respect to the incoming beam is often used to accelerate the alignment. Throughout this paper we will focus on linear two mirror cavities. Some of the following formulas would have to be slightly modified for triangular three mirror cavities. We also ignore a few effects that do not change the outcome of our research such as the Guoy phase of the spatial Hermite-Gauss eigenmodes of the optical cavities. The interested reader is referred to [8] for detailed information about different resonator types and the properties of their spatial eigenmodes.

Optical cavities are characterized by their free spectral range (FSR):

$$FSR = \frac{c}{2L}\,, \tag{4}$$

where L is the distance between mirrors, and their finesse:

$$F = \frac{\pi\sqrt{r_1 r_2}}{1 - r_1 r_2} \overbrace{\approx}^{r_1 = r_2} \frac{\pi}{T}\,, \tag{5}$$

r_1 and r_2 are the amplitude reflectivities of the cavity mirrors, T is the intensity transmissivity of each of the mirrors. The laser field is resonant in the cavity when the round trip phaseshift is a multiple of 2π. Each cavity has a series of resonances separated by the FSR:

$$\frac{\nu_n}{FSR} = n \qquad n \,\varepsilon\, \aleph\,. \tag{6}$$

The width of the resonance is usually given in terms of the Full-Width Half Maximum (FWHM) or Half-Width Half Maximum (HWHM). These values are correlated with the FSR and the finesse as follows:

$$FWHM = \frac{FSR}{F} = 2 \cdot HWHM\,. \tag{7}$$

The goal of the laser frequency stabilization system is to ensure that the laser frequency is close to one of the resonances of the cavity and that the difference changes by less than the required frequency stability. In LISA, this would require a relative stability of $30\,\mathrm{Hz}/\sqrt{\mathrm{Hz}}$ over 1000 s of the laser frequency with respect to the cavity resonance frequency, assuming that the cavity resonance frequency has stability better than $30\,\mathrm{Hz}/\sqrt{\mathrm{Hz}}$.

3 Experimental Setup

A standard technique to stabilize the laser frequency is an *rf* reflection locking technique (Pound-Drever-Hall [6]). This technique is extensively discussed in the literature (see for example [9]) and will not be discussed in this paper. We set up two nearly identical and

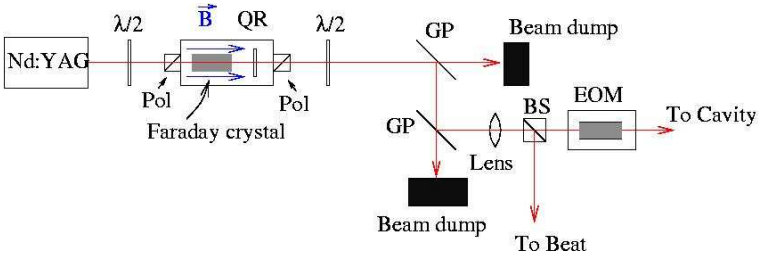

Figure 1: The first part of the experimental setup: The laser beam passes through an optical Faraday isolator. After the isolator, most of the laser power is dumped and the remaining few milliwatts are phase-modulated by the EOM.

Actuator	Tuning Range	Bandwidth	Tuning Coefficient
PZT	100 MHz	≈ 100 kHz	≈ 5 MHz/V
Temperature	10 GHz	0.1 Hz	≈ 3 GHz/V

Table 1: Tuning ranges, bandwidth, and coeffcients of the laser frequency actuators.

independent systems to compare with each other. Our experimental setup consists of two diode pumped Nd:YAG Non-Planar Ring Oscillator (NPRO) lasers with maximum output power of 700 mW. We operated the lasers at approximately 500 mW output power. These lasers have internal intensity servos that stabilize the laser intensity from approximately 1 Hz to several hundred kHz. Its main function is to suppress the relaxation oscillations. It is important to notice that the intensity servos are not stabilizing the laser intensity below 1 Hz.

A PZT with 100 kHz bandwidth is used as a fast frequency actuator. This actuator has a dynamic range of ~ 100 MHz. The temperature of the laser crystal is used as the slow frequency actuator, and has a large dynamic range (about 10 GHz). Table 1 summarizes the properties of both frequency actuators[1].

Two wave plates and one optical isolator follow the laser head (see Fig. 1). The first half wave plate is used to rotate the polarization of the laser to match the transmitting polarization of the optical isolator. The second half wave plate is used to optimize the polarization for the electro-optic modulator (EOM) to minimize residual polarization and amplitude modulation (see Section 4). The glass plates reflect only a small amount of power and most of the laser power is dumped into the two beam dumps. The photo detectors used in the experiment only have a limited linear power range of 1 mW. This arrangement reduces the power through the EOM to about 2.5mW (see Figure 2}). The phase modulated (modulation index m ≈ 0.1) and linearly polarized field is reflected at the polarizer cube and passes through a quarter wave plate, followed by two lenses to mode match the laser field to the spatial eigenmode of the cavity. The cavity parameters for the two different cavities are given in table 2[2].

Each cavity rests in its own vacuum chamber and is surrounded by five layers of gold

[1]Tuning coefficients are small signal coefficients. They depend on the specific laser and the actual tem-

	Length	FSR	Finesse	R_1	R_2
Cavity 1	25.08 cm	597.65 MHz	10150 ± 1000	inf	0.5 m
Cavity 2	18.968 cm	790.25 MHz	9744 ± 1000	0.5 m	0.5 m

Table 2: The parameters of the two cavities: R_1, R_2 are the radii of curvature of the two cavity mirrors. The nominal transmission of all cavity mirrors is T = 250 ppm. This would result in a nominal finesse of 12566. The measured finesse of around 10000 corresponds either to a transmission of T = 300 ppm or additional round trip losses due to scattering and absorption at the mirrors of about 100 ppm.

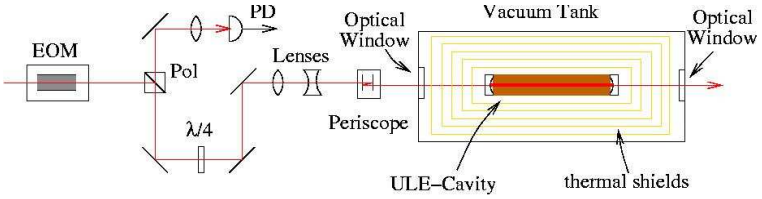

Figure 2: The second part of the experimental setup: The light after the modulator is steered and mode matched into the ULE cavity which sits inside the thermally shielded vacuum tank.

coated stainless steel plates, separated by Macor stand-offs (See Fig. 3).The gold reflects thermal radiation, while the stainless steel holds the gold and ensures the mechanical stability of the design. The only two clear lines of sight to the cavity are through the optical windows at the front and back of the vacuum chamber. The field, which is reflected from the cavity input mirror, passes again through the lenses and the quarter wave plate. Depending on the rotation of the quarter wave plate, parts of the reflected field transmit through the polarizer and is then detected with the fast photo detector (New Focus 1611 AC-FS). During lock acquisition, the entire 2.5 mW (1.5 mW for the second laser) are reflected. We reduce the power on the photo detector by rotating the quarter wave plate to ensure linear behavior of the photo detector. After lock is acquired, 70 to 90% of the power is transmitted through the cavity and we rotate the quarter wave plate such that all the reflected light is detected by the photodetector. Depending on the mode matching about 200 to 400 μW of laser light is on the photo detectors during lock.

In the early stages of the experiments, the AC component of the photocurrent was demodulated directly with a 7 dBm double balanced mixer. Later, an RF-amplifier was added (Texas Instrument: THS4021) that amplified the signal by an additional factor of 10.

After adding the amplifiers the measured slopes of the demodulated error signal were measured to be:

$$\frac{dV}{df} = 67 \frac{\mu\text{V}}{\text{Hz}} \qquad \text{firstlaser,} \tag{8}$$

perature, but both values are good approximations at all ranges.

[2]Length calculated from measured FSR.

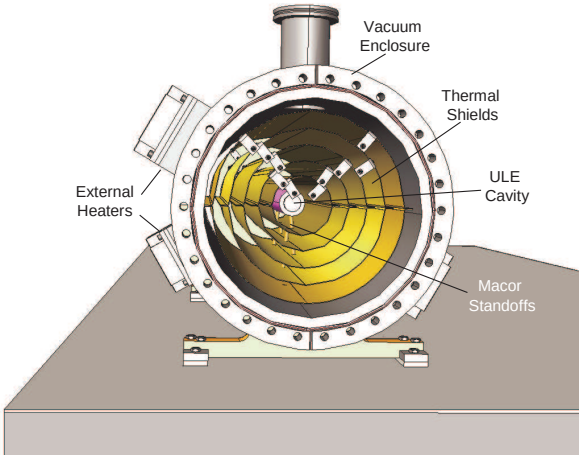

Figure 3: Drawing of ULE frequency reference cavity housed in five layers of gold coated stainless steel thermal shields. Note, the end caps of thermal shields and vacuum tank are not shown.

$$\frac{dV}{df} = 23.3\,\frac{\mu\mathrm{V}}{\mathrm{Hz}} \qquad \text{secondlaser.} \tag{9}$$

The difference in the slopes of the error signals is caused by the difference in the linewidth, differences in the optical efficiency, and differences in the modulation index in the two setups. However, these slopes change over time, possibly by as much as 50%. One reason is changes in the visibility. The first laser had, at best times, a visibility of $\approx 90\%$; the second laser $\approx 85\%$ at best. This visibility was not sustained all the time, or even kept constant, as the alignment drifted over long time scales. As a consequence many experiments were run with visibilities around 70%. Also, drifts in the resonance frequency of the EOM changes the modulation index over time.

These error signals were then amplified and used to lock the frequency of each laser to its reference cavity. The two laser fields then beat against each other and the difference frequency is measured every 2 s by a fast counter and recorded with a computer.

4 Noise Sources

It is conceptually reasonable to distinguish between technical noise in the read out system and optical path length (OPL) changes in the reference cavity. For example, tilt locking [10] could be used as an alternative read out system to the PDH-system described in this paper. Such a change would only affect the technical noise in the read out system and has virtually no influence on the OPL changes. On the other hand, other spacer materials like Zerodur or Clearceram-Z and alternative bonding techniques like hydroxy-catalysis bonding [11] will not, or only to a small degree, change the scaling of technical noise into frequency noise. We will briefly discuss optical path length changes in the reference cavity and then focus on technical noise associated with the read out system.

4.1 Stability of Reference Cavity

4.1.1 Laser Independent Changes

The most obvious source for possible length changes of the reference cavity are temperature induced changes. The gold-coated thermal-shields inside the vacuum chamber will suppress ambient temperature fluctuations by several orders of magnitude. In addition to the insulation, the cavity material itself will average over spatial inhomogeneities in the temperature fluctuations and the thermal mass of the cavity will low pass filter the fluctuations furthermore. Based on the results presented in the following chapter, we assume that the temperature fluctuations of the cavity material itself are smaller than a few $\mu\mathrm{K}/\sqrt{\mathrm{Hz}}$ over the LISA measurement band.

It is also well known that materials like ULE or Zerodur shrink slowly over time. This creep is sometimes thought to be a series of single spontaneous relaxation processes inside the material. If this is the case, then it is reasonable to assume that the associated noise depends on the history of the material, how it was produced and especially how and when it was machined. Also, the bonds between the mirrors and the spacer can change over time depending on the type of bond and the surface quality. The long term goal of our experiments is to gain at least an empirical understanding how the machining and bonding history of the cavities influences their stability.

4.1.2 Length Fluctuations Through Laser Intensity Noise

Parts of the laser field will be absorbed in the substrates and coatings of the mirrors. This will increase the temperature of the mirrors and subsequent thermal expansion will change the resonance frequency of the cavity. The circulating power inside the cavity is

$$P_{cav} = \frac{P_{in}}{T} \approx 10\,\mathrm{W}\frac{P_{in}}{[2.5\,\mathrm{mW}]}\,. \tag{10}$$

We estimate the absorption coefficient of the coatings inside the cavity to be 10 ppm. Under this assumption, each mirror would absorb

$$P_{abs}^{coat} = 100\,\mu\mathrm{W}. \tag{11}$$

The local expansion across the beam profile would then be [12]:

$$\Delta s = \frac{\alpha}{4\pi\kappa} P_{abs}^{coat}\,, \tag{12}$$

where α is the thermal expansion coefficient and κ is the heat conductivity of the substrate material. For the fused silica mirrors used in this experiment:

$$\frac{\alpha}{\kappa} = 3.7\cdot 10^{-7}\,\frac{\mathrm{m}}{\mathrm{W}} \qquad \alpha_{FS} = \frac{5.1\cdot 10^{-7}}{\mathrm{K}} \qquad \kappa_{FS} = 1.38\,\frac{\mathrm{W}}{\mathrm{mK}}\,. \tag{13}$$

The local expansion is then:

$$\Delta s = \frac{3.7\cdot 10^{-7}\,\mathrm{m}}{4\pi\,\mathrm{W}}\cdot 100\,\mu\mathrm{W} \approx 2.9\,\mathrm{pm}, \tag{14}$$

which changes the resonance frequency of the long cavity by:

$$\Delta\nu \approx 2 \cdot \nu \frac{\Delta s}{L} = 6.5\,\mathrm{kHz}, \tag{15}$$

while the resonance frequency of the short cavity will change by:

$$\Delta\nu \approx 2 \cdot \nu \frac{\Delta s}{L} = 8.6\,\mathrm{kHz}. \tag{16}$$

The factor 2 takes into account that both mirrors expand. This deformation, localized only across the laser beam, is a result of the limited heat conductivity of the mirror substrates. These substrates will also experience a nearly homogeneous expansion generated by the nearly homogeneous temperature increase across the entire mirror substrate. This expansion is directed outward and will in first order not change the optical path length between the mirror coatings.

Finally, the heat also increases the temperature of the cavity spacer. In addition to the light absorbed in the coatings, additional light will also scatter at the surfaces of the mirrors and will be absorbed in the spacer. Based on the measured finesse, we estimate that no more than 100 ppm or 1 mW of the cavity internal field is lost at the two mirrors and will be absorbed in the spacer.

In equilibrium the entire heat generated by the laser field has to be radiated into the environment. We use the black body radiation to estimate the temperature increase. The radiation of a black body at a certain temperature is:

$$R_{cav\to tank} = 5.7 \cdot 10^{-8} \frac{\mathrm{W}}{\mathrm{m^2 K^4}} T_{cav}^4. \tag{17}$$

At the same time the environment or tank radiates heat back to the cavity:

$$R_{tank\to cav} = 5.7 \cdot 10^{-8} \frac{\mathrm{W}}{\mathrm{m^2 K^4}} T_{tank}^4. \tag{18}$$

The net heat exchange has to be equal to the absorbed power ($\approx 1\,\mathrm{mW}$):

$$(R_{cav\to tank} - R_{tank\to cav}) \cdot A = R_{tot} \cdot A = 5.7 \cdot 10^{-8} \frac{\mathrm{W}}{\mathrm{m^2 K^4}} 4 \cdot T_{tank}^3 \Delta T \cdot A \approx 1\,\mathrm{mW}. \tag{19}$$

The surface area, A, of the long cavity is

$$A_l = 2\pi r l \approx 2\pi \cdot 0.015\,\mathrm{m} \cdot 0.3\,\mathrm{m} \approx 0.028\,\mathrm{m^2}, \tag{20}$$

while the short cavity has a surface area of

$$A_s = 0.018\,\mathrm{m^2}. \tag{21}$$

The temperature of the tank will be around 300 K. The temperature of the long cavity will then increase by

$$\Delta T \approx 6.9\,\mathrm{mK}, \tag{22}$$

Location Time scale	Surfaces Instantaneous	Spacer Low pass filtered	Spacer Time Constant
Long Cavity	$6.6\,\mathrm{kHz}\frac{P_{abs}^{coat}}{[100\,\mu\mathrm{W}]}$	$38\,\mathrm{kHz}\frac{P_{abs}}{[1\,\mathrm{mW}]}$	$2.0\cdot10^4\,\mathrm{s}$
Short Cavity	$8.7\,\mathrm{kHz}\frac{P_{abs}^{coat}}{[100\,\mu\mathrm{W}]}$	$51\,\mathrm{kHz}\frac{P_{abs}}{[1\,\mathrm{mW}]}$	$1.2\cdot10^4\,\mathrm{s}$

Table 3: Expected laser induced length changes of the two cavities.

and the temperature of the short cavity will increase by:

$$\Delta T \approx 9\,\mathrm{mK}. \tag{23}$$

This temperature increase expands both cavities by:

$$\Delta L = L\cdot\alpha_{ULE}\cdot\Delta T \leq 34\,\mathrm{pm} \qquad \alpha_{ULE} \leq \frac{2\cdot10^{-8}}{\mathrm{K}}, \tag{24}$$

and changes the resonance frequency of the long cavity by

$$\Delta\nu \leq \nu\frac{\Delta L}{L} \approx 38\,\mathrm{kHz}, \tag{25}$$

and of the short cavity by

$$\Delta\nu \leq \nu\frac{\Delta L}{L} \approx 51\,\mathrm{kHz}. \tag{26}$$

Fluctuations of the laser intensity should be seen instantaneously (compared to periods of LISA signals) in the surface heating of the mirror while the thermal mass of the cavity spacer will act as a low pass filter. The time constant of the ULE spacers can be approximated by:

$$\tau = \frac{q}{\kappa}\rho\left(\frac{L}{2}\right)^2, \tag{27}$$

with $q = 776\,\mathrm{J/kg/K}$(specific heat), $\kappa = 1.31\,\mathrm{W/m/K}$ (thermal conductivity), and $\rho = 2210\,\mathrm{Kg/m^3}$(density) of ULE. L is the length of the spacer. This model assumes that the absorption takes place on the mirror surfaces. However parts of the scattered light will be absorbed along the entire cavity material causing a more uniform heating process. Subsequently, we probably overestimate the time constant of the spacer material. A summary of the expected laser induced length changes is shown in Table 3.

Each of these values should be taken with great care as this is only a very rough thermal model. We may overestimate the amount of scattered light (absorbed in the spacer) as well as the absorption coefficient in the coatings (surfaces) by up to one order of magnitude. However, based on these values we can assume that both processes contribute roughly equally to length changes in the LISA frequency band and that both processes have to be considered. The frequency noise requirements of $30\,\mathrm{Hz}/\sqrt{\mathrm{Hz}}$ in the LISA band set an upper limit on the relative intensity noise of the laser:

$$\mathrm{RIN} < \frac{3\cdot10^{-2}}{\sqrt{\mathrm{Hz}}} \qquad \text{at } 3\ \mathrm{mHz}. \tag{28}$$

It should be noted that the requirements on the relative intensity noise of the LISA lasers of $10^{-4}/\sqrt{\mathrm{Hz}}$ over the LISA band is based on unrelated effects.

Freq.	1 mHz	3 mHz	10 mHz	30 mHz
short cavity	$17\,\mathrm{Hz}\cdot\frac{dI/I}{[10^{-2}]}$	$10\,\mathrm{Hz}\cdot\frac{dI/I}{[10^{-2}]}$	$7\,\mathrm{Hz}\cdot\frac{dI/I}{[10^{-2}]}$	$10\,\mathrm{Hz}\cdot\frac{dI/I}{[10^{-2}]}$
long cavity	$25\,\mathrm{Hz}\cdot\frac{dI/I}{[10^{-2}]}$	$20\,\mathrm{Hz}\cdot\frac{dI/I}{[10^{-2}]}$	$20\,\mathrm{Hz}\cdot\frac{dI/I}{[10^{-2}]}$	$20\,\mathrm{Hz}\cdot\frac{dI/I}{[10^{-2}]}$

Table 4: Frequency variations of the two cavities due to laser power variations at different frequencies.

4.2 Intensity Noise and Frequency Fluctuations

We modulated the intensity of one of the laser fields and monitored the subsequent frequency changes. The setup was as follows: Both lasers were locked to their respective cavity. We modulated the intensity of one of the lasers through its intensity modulation input and recorded:

1. the beat frequency
2. laser intensities
   (a) in front of the cavities
   (b) transmitted through the cavities
3. actuator signals
   (a) PZT
   (b) Temperature

The modulation of the intensity of both lasers led to the results presented in Table 4.

Errorbars on these measurements are approximately in the 10 to 20% range. In addition, drifts in the alignment and in offsets will also change the intensity noise to frequency noise coupling over time. A measurement of the intensity noise at these low frequencies is non-trivial. The standard procedure is to measure the intensity with a photo receiver, transform the photocurrent into a voltage and subtract this signal from a constant voltage generated by a stable voltage reference. One of the limitations of this measurement are the fluctuations in the voltage reference. We were so far only able to put an upper limit of about $5\cdot 10^{-3}/\sqrt{\mathrm{Hz}}$ at 3 mHz on the laser intensity noise. Again, we do not believe that the noise level is stationary over all measurement times. For example, the alignment of spurious interferometers formed between different optical components (for example inside the EOM) will change with room temperature. It is also important to note that this is only the laser intensity in front of the cavity. The above described effect couples to the changes in the intensity inside the cavity, not to the changes in the power in front of the cavity. But changes in the alignment due to temperature or pressure changes in the laboratory will change the mode matching efficiency and hence will change the power build up in the cavity without changing the power in front of the cavity.

In addition, we were not able to correlate the intensity noise very well with the frequency fluctuations. Therefore, it is probably only safe to say that intensity fluctuations are one possible noise source which limit our stability but it is not clear that they are the limiting noise source.

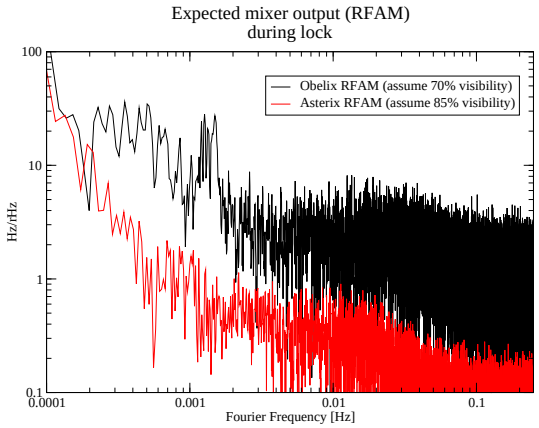

Figure 4: The expected frequency noise calculated from the measured RFAM of the two lasers. As the coupling depends on the mode matching and alignment it is expected that this frequency noise contribution changes over time.

4.3 Radio Frequency Amplitude Modulation (RFAM)

Electro-optic modulators not only modulate the phase of the electric field but also the polarization. A polarizer following the modulator will transform the latter into amplitude modulation. This amplitude modulation can be described as:

$$I_{RFAM} = I_o(1 + 2M cos\Omega t) \tag{29}$$

where M is the amplitude modulation index, and I_o is the intensity of the laser field through the modulator. Changes in the amplitude modulation will change the laser frequency by:

$$\delta\nu = HWHM\frac{\delta M}{m} \approx \frac{40\,\mathrm{kHz}}{\sqrt{\mathrm{Hz}}}\frac{\delta M}{m} \tag{30}$$

where m is the phase modulation index. Changes in the amplitude modulation index of the order $\delta M = 10^{-4}$ would generate frequency noise at the level of $40\,\mathrm{Hz}/\sqrt{\mathrm{Hz}}$. Figure 4 shows a graph of the measured RFAM generated frequency noise for the two laser systems.

4.4 Electronic Noise in the Read Out System

The noise in the photo detectors is specified to be about $20\,\mathrm{pW}/\sqrt{\mathrm{Hz}}$ or $16\,\mathrm{pA}/\sqrt{\mathrm{Hz}}$. The transimpedance of the photodetector of $700\,\Omega$ transforms this to about $11\,\mathrm{nV}/\sqrt{\mathrm{Hz}}$. The input-referred noise of the RF-Amplifier is also in this range. This has to be compared with the $4.7\,\mu\mathrm{V/Hz}$ slope of the (non-amplified) errorsignal. Electronic noise in the RF path should create frequency noise in the order of a few $\mathrm{mHz}/\sqrt{\mathrm{Hz}}$, about three orders of magnitude below the LISA requirements.

Changes in the electronic offsets at the mixer output, U_{mixer}, or the input of the first amplifier, U_{DC}, would change the laser frequency by

$$\delta\nu \approx 40\,\frac{\delta U_{DC} + \delta U_{mixer}}{[\mathrm{mV}]}\,\frac{\mathrm{Hz}}{\sqrt{\mathrm{Hz}}}. \tag{31}$$

Spectral densities of the voltage noise are usually not available in the LISA band. A rough estimate of the noise based on specifications for offset drifts indicate that this may be one of our main noise sources. However, if this is the limiting noise source, the frequency fluctuations should scale with the inverse gain of the RF-amplifier. This was not the case.

DC-offsets in the error signal can be caused by offsets in the mixer output or offsets in the first amplifier. These offsets will offset the laser frequency from the resonance frequency of the cavity by

$$\Delta\nu = \frac{df}{dV}\Delta U\,, \tag{32}$$

or

$$\Delta\nu \approx \frac{15\,\mathrm{Hz}}{\mathrm{mV}}\Delta U \qquad \text{first Laser,} \tag{33}$$

$$\Delta\nu \approx \frac{43\,\mathrm{Hz}}{\mathrm{mV}}\Delta U \qquad \text{second Laser.} \tag{34}$$

Here we used the measured slopes of our error signals. Offsets in the order of a few millivolts or a few 100 Hz are expected, but the fluctuations should be well below $1\,\mathrm{mV}/\sqrt{\mathrm{Hz}}$. Changes in the laser intensity will change the slope of the error signal and subsequently, the DC-offset induced frequency offset. In the preceding section, we derived a limit on the relative intensity noise (RIN) of $3\cdot 10^{-2}/\sqrt{\mathrm{Hz}}$ for our experiment. Such a RIN-level would allow DC-offsets in the vicinity of a few hundred millivolts without sacrificing the frequency stability of the laser.

4.5 Laser Fluctuations

A laser field has several degrees of freedom. Our stabilization system is aiming to stabilize the frequency of the field. The other degrees of freedom are the polarization, the intensity, and the spatial mode or the propagation direction. Changes in the polarization will only manifest itself as changes in the intensity of the laser field and can be included in the earlier discussions. The detection scheme is only in second order sensitive to changes in the propagation direction or pointing of the laser beam. Pointing to frequency noise coupling requires a static misalignment of the laser cavity with respect to the laser beam. This has been discussed in many publications associated with ground based gravitational wave detectors (see for example [13]).

The basic idea is that a misaligned cavity couples the fundamental and the first order Hermite-Gauss mode of the laser. Any first order mode content in the laser beam will then be transferred back into the fundamental mode at the misaligned cavity. The phase of this contribution is different from the phase of the original fundamental mode inside the cavity. This is equivalent to an apparent change in the round trip phase inside the cavity. The magnitude of the static misalignment can be approximated based on the on resonance visibility or the ratio between the transmitted intensities of the TEM00-mode and the TEM10-mode. A static tilt of $\Theta = 10^{-5}$rad would reduce the visibility in the short cavity by 20% and in the long cavity by 12%. Most of this light would be in the TEM10-mode. Most of the time the tilt should have been closer to the 10^{-6} rad level as the TEM10-mode is easy to reduce during the alignment and 10^{-5} rad can be considered an upper limit for the static tilt during long data runs.

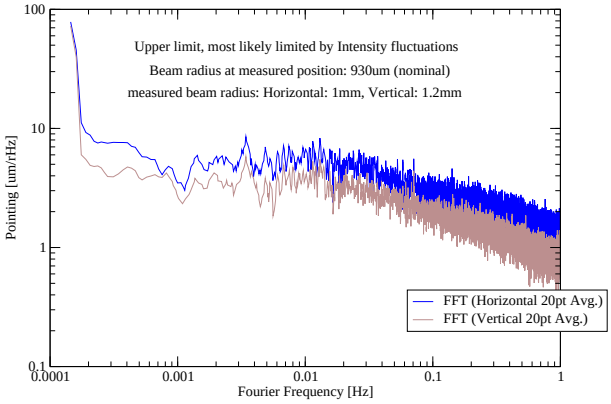

Figure 5: The measured pointing of the two laser beams is in the order of $0.01/\sqrt{\text{Hz}}$ of the beam waist. This is equivalent to a relative amplitude of the 10-mode in the order of $0.01/\sqrt{\text{Hz}}$ of the fundamental mode.

The pointing to frequency noise coupling is then approximately:

$$\delta\nu_{Pointing} \approx \frac{\Theta}{[10^{-5}\text{rad}]} \cdot \frac{a_{10}}{[0.1/\sqrt{\text{Hz}}]} \cdot 30\frac{\text{Hz}}{\sqrt{\text{Hz}}} \qquad \text{long cavity,} \tag{35}$$

$$\delta\nu_{Pointing} \approx \frac{\Theta}{[10^{-5}\text{rad}]} \cdot \frac{a_{10}}{[0.1/\sqrt{\text{Hz}}]} \cdot 40\frac{\text{Hz}}{\sqrt{\text{Hz}}} \qquad \text{shortcavity.} \tag{36}$$

An amplitude of $0.1/\sqrt{\text{Hz}}$ in the TEM10-mode (or intensity of $1\%/\sqrt{\text{Hz}}$) due to pointing in the laser beam would cause frequency fluctuations of 30-40 $\text{Hz}/\sqrt{\text{Hz}}$ if the cavity misalignment is in the 10^{-5} rad range. The amplitude of the TEM10-mode is always within the 1% range (see Fig. 5) which indicates that pointing induced frequency fluctuations are about an order of magnitude below LISA requirements.

4.5.1 Pointing at the Photo Detector

Pointing of the laser beam into the photo detector is another possible coupling mechanism through which the frequency of the laser could change. It can change the intensity dependent offsets caused by offset locks or RFAM (see above). This is identical to the frequency fluctuations caused by intensity fluctuations of the laser itself except for the case where intensity fluctuations change the temperature of the cavity mirrors.

5 Final Frequency Noise

5.1 The 30 Day Run

After installing all optical, vacuum, and electronic components (except for the RF-amplifier), we started a long data run. At that time, one of the lasers was already locked to its cavity for a few days while we were still working on the feedback and alignment of the second

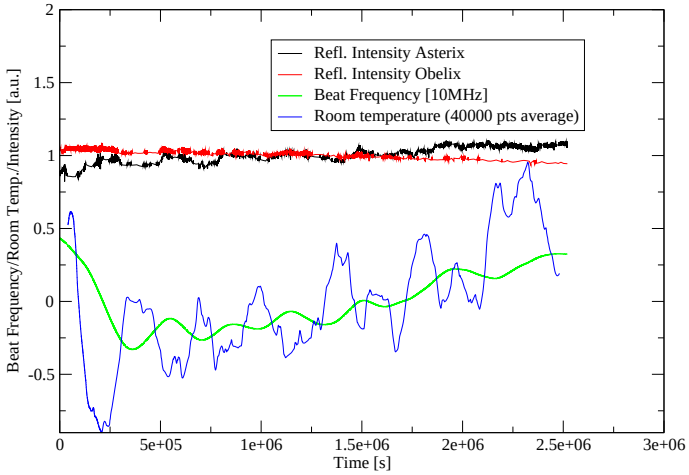

Figure 6: The time series of the frequency of the beat signal, the room temperature, and the reflected intensities are shown. The correlation between frequency and temperature changes is obvious.

laser. It can be assumed that the first cavity was in thermal equilibrium when we started the measurement. The time series is shown in Fig. 6}. We lost lock twice during the first two days for a few minutes while we were still working around the optical table. The reason for the following increase in the beat signal frequency and the oscillations with 4 day period can be correlated to the room temperature. Changes in the room temperature change the beat frequency with a delay of about 140000 s or 1.7 days. The reflected intensity, which is a measure of the visibility or alignment is also changing over time.

The entire data set was chopped into smaller time series with 2^{16} data points, allowing the use of fast FFT tools. A quadratic fit was subtracted from each time series to take out the linear and quadratic drift terms. After these modifications a Hanning filter was used before performing the FFTs. The spectral densities of the frequency fluctuations for four typical time series are shown in Fig. 7. The noise is non-stationary especially at frequencies below 10 mHz. However, the 1/f characteristic in the blue curve is most likely caused by limited sideband suppression of some very low frequency noise component.

The shown spectral densities are the rms-frequency fluctuations of the beat signal. Under the assumption that both lasers have the same noise, these densities should be divided by a factor $\sqrt{2}$ to get the rms-frequency fluctuations of each laser. However, the requirements for LISA are specified as amplitudes of the frequency fluctuations. The difference is again a factor of $\sqrt{2}$ which compensates the first factor.

5.2 With RF-Amplifier

One possible noise source which could have limited us was electronic noise after the demodulation. There are essentially two ways to reduce the problem. One is to reduce the noise at that knot, the second possibility is to increase the signal before the demodulation. We decided to follow the second possibility and amplified the RF-signal from the photo

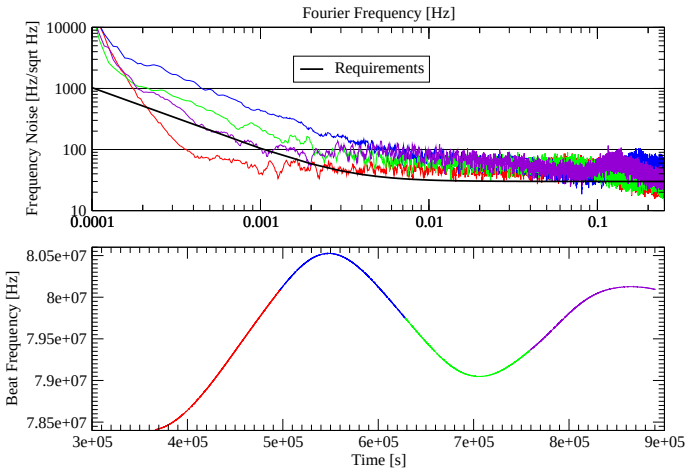

Figure 7: The frequency noise for various parts of the 30 day data run (upper graph) and the time series (lower

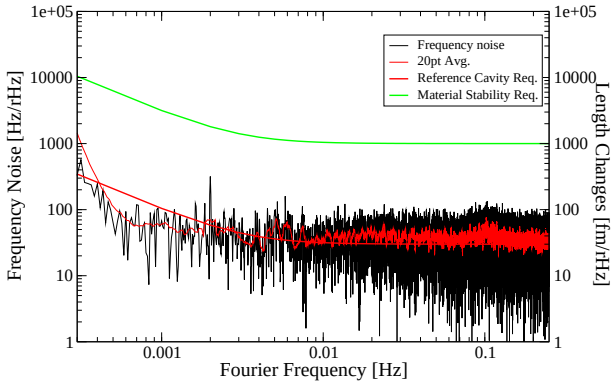

Figure 8: The noise after inserting the RF amplifier.

detector with an RF-amplifier. The problem with this setup is that during lock acquisition, the RF-signal was so large that it saturated the mixer. For lock acquisition, we turned the quarter wave plate between the cavity and the polarizer and reduced the signal on the photo detector. After we acquired lock, we turned the quarter wave plate back into its optimum position and worked with the maximum signal.

The first measured frequency noise after this change is shown in Fig. 8. This change reduced the frequency noise immediately to about $40\,\mathrm{Hz}/\sqrt{\mathrm{Hz}}$ at Fourier frequencies above 1 mHz.

5.3 Final Result and Interpretation

Later measurements showed even better performances which met the LISA requirements (see Fig. 9). All future measurements have given very similar results: the frequency fluctuations were always at least below the $40\,\mathrm{Hz}/\sqrt{\mathrm{Hz}}$ level, most of the time below the LISA

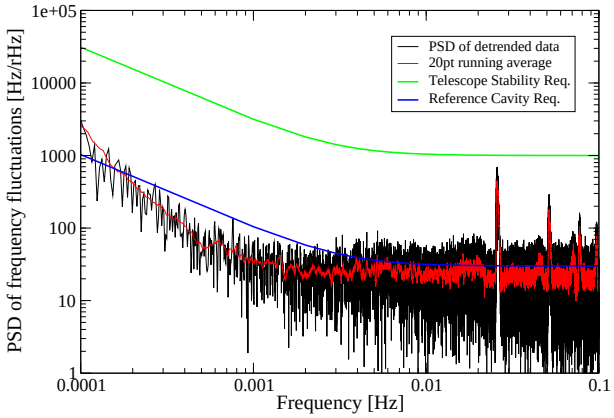

Figure 9: The frequency noise during the latest runs.

requirements with the exception of small frequency bands around the cross over between temperature and PZT feedback. However, the measured noise floors can not be explained completely by any of our analyzed and characterized noise sources. It may be the sum of all noise sources or, are real length fluctuations in the cavity material with occasional significant contributions of RFAM and laser intensity noise. These contributions seem only relevant if spurious interferometers in the laser path become significant.

Usually, the spectrum is nearly white at frequencies above 0.4 mHz. It is unlikely that these "white" changes can be correlated to temperature changes in the ULE material. These changes should have a time constant which should force the spectrum to roll down at higher frequencies. If this is really caused by the cavity material itself, one possible explanation would be spontaneous processes in the material. Stress might have been built up during machining and polishing of the ULE rods. This stress might be released through spontaneous reordering processes inside the glass. It can be assumed that these stress relaxation processes are independent from each other. A large enough rate could generate a white spectrum.

If this is really the limiting noise source, it might be reasonable to expect further decreases in the frequency noise over time.

References

[1] Astrium GmbH, *LISA - Final Technical Report*, ESTEC Contract No. 13631/99/NL/MS, Report No. **Li-RP-DS-009** (2000).

[2] Daniel A. Shaddock, Massimo Tinto, Frank B. Estabrook, J.W. Armstrong, *Data combinations accounting for LISA spacecraft motion*, Phys. Rev. D **68**, 061303(R) (2003).

[3] Corning Inc, *Corning Code 7972 ULE*, See: http://www.corning.com/ semiconductoroptics/products_services/semiconductor_optics/ule.asp

[4] Schott AG, *Zerodur*, See: http://www.us.schott.com/optics_devices/english/products/zerodur/

[5] Ohara Inc, *Clearceram-Z*, See: http://www.ohara-inc.co.jp/b/b02/b0210_cz/b0210.htm

[6] R.W.P. Drever, J.L. Hall, F.V. Kowalski, J. Hough, G.M. Ford, A.J. Munley, Laser phase and frequency stabilisation using optical resonator *Appl. Phys. B*, **31**, (1983).

[7] Many publications deal with this subject. Optical cavities are discussed for example in Miao Zhu, John L. Hall, Short and Long Term Stability of Optical Oscillators, *IEEE Frequency Control Symposium*, pp. 44-55 (1992). Iodine-stabilized lasers are discussed in A.Yu Nevsky et al., Frequency comparison and absolute frequency measurement of I_2-stabilized lasers at 532nm, *Opt. Comm.* **192** (2001) 263-272.

[8] A.E. Siegman *Lasers* University Science Books, Mill Valley (1986).

[9] A. Schenzle, R.G. DeVoe, R.G. Brever, Phase-modulation laser spectroscopy, *Phys.Rev. A*, **25**, 2606 (1981).

[10] B. Slagmolen, D. Shaddock, M. Gray, D. McClelland, Frequency Stability od Spatial Mode Interference (Tilt) Locking, *IEEE J. of Quantum Electronics*, **38**, 11, (2002).

[11] Gwo, D.-H., *Ultra precision and reliable bonding method.* United States Patent No. US 6284085 B1 (2001).

[12] W. Winkler, K. Danzmann, A. Rüdiger, R. Schilling, Heating by optical asbsorption and performance of interferometris gravitational wave detectors, *Physical Review A*, **44**, 11 (1991)

[13] Y. Hefetz, N. Mavalvala, D. Sigg, *Principles of calculating alignment signals in complex resonant optical interferometers*, LIGO-T960024-A-D (1996). See also Daniel Siggs papers: The Modal Model available in the LIGO document center: www.ligo.caltech.edu.

REPORT DOCUMENTATION PAGE

Form Approved
OMB No. 0704-0188

1. REPORT DATE *(DD-MM-YYYY)*	2. REPORT TYPE	3. DATES COVERED *(From - To)*
07-12-2005	Technical Memorandum	

4. TITLE AND SUBTITLE

Laser Frequency Stabilization for LISA

5a. CONTRACT NUMBER

5b. GRANT NUMBER

5c. PROGRAM ELEMENT NUMBER

6. AUTHOR(S)

Guido Mueller
Paul McNamara
Ira Thorpe
Jordan Camp

5d. PROJECT NUMBER

5e. TASK NUMBER

5f. WORK UNIT NUMBER

7. PERFORMING ORGANIZATION NAME(S) AND ADDRESS(ES)

NASA/Goddard Space Flight Center
Code 663
Greenbelt, MD 20771

8. PERFORMING ORGANIZATION REPORT NUMBER

2006-00387-1

9. SPONSORING/MONITORING AGENCY NAME(S) AND ADDRESS(ES)

National Aeronautics and Space Administration
Washington, DC 20546-0001

10. SPONSORING/MONITOR'S ACRONYM(S)

11. SPONSORING/MONITORING REPORT NUMBER

TM-2005-212794

12. DISTRIBUTION/AVAILABILITY STATEMENT

Unclassified-Unlimited, Subject Category: 42
Report available from the NASA Center for Aerospace Information,7121 Standard Drive, Hanover, MD 21076. (301) 621-0390

13. SUPPLEMENTARY NOTES

Guido Mueller and Ira Thorpe, Department of Physics, University of Florida, Gainesville, Florida

14. ABSTRACT

The requirements on laser frequency noise in the Laser Interferometer Space Antenna (LISA) depends on the velocity and our knowledge of the position of each spacecraft of the interferometer. Currently it is assumed that the lasers must have a pre-stabilized frequency stability of 30 Hz/the square root of Hz over LISA's most sensitive frequency band (3mHz - 30 mHz). The intrinsic frequency stability of even the most stable commericial lasers is several orders of magnitude above this level. Therefore it is necessary to stabilize the laser frequency to an ultra-stable frequency reference which meets the LISA requirements. The baseline frequency reference for the LISA lasers are high finesse optical cavities based on ULE spacers. We measured the stability of two ULE spacer cavities with respect to each other. Our current best results show a noise floor at, or below, 30 Hz/the square root of Hz above 3mHz. In this report we describe the experimental layout of the entire experiment and discuss the limiting noise sources.

15. SUBJECT TERMS

LISA, laser frequency stabilization, lasers

16. SECURITY CLASSIFICATION OF:			17. LIMITATION OF ABSTRACT	18. NUMBER OF PAGES	19b. NAME OF RESPONSIBLE PERSON
a. REPORT	b. ABSTRACT	c. THIS PAGE			Jordan Camp
Unclassified	Unclassified	Unclassified	Unclassified	17	19b. TELEPHONE NUMBER *(Include area code)* (301) 286-3528